DI-14

DEFORMATION BEHAVIOR AND FRACTURE OF NIMONIC 80A DURING THERMAL FATIGUE CYCLING UNDER CONSTRAINT

Erhard Krempl*

ABSTRACT

Thermal fatigue tests on solid cylindrical specimens were performed by restraining their thermal expansion at the maximum or the minimum cycle temperature in two clamping frames of different stiffnesses. The behavior of each specimen throughout its life was monitored by reading temperature-reaction force hysteresis loops automatically at preset intervals.

The stiffness of the clamping frame influences the stresses and strains at the set-up cycle. During cycling specimens tend to reach shake-down stresses. The shake-down conditions are completely elastic or equal plastic deformation at the maximum and minimum cycle temperature. They are therefore not only dependent on the initial conditions (temperature, degree of restraint, virgin material properties) but also on the changes of the material properties due to thermal cycling (strain-hardening or softening). Equilibrium is not necessarily reached at a zero mean stress but rather at a tensile mean stress.

Cycles-to-failure curves can be based on independent and on dependent test variables. The significance of this differentiation is discussed and demonstrated. Of all the quantities measured, only the width of the loop at the end of the first cycle, a dependent test variable, yields one cycles-to-failure curve.

* Materials and Processes Laboratory, General Electric Company, Schenectady, N.Y., U.S.A., formerly with Technische Hochschule Muenchen, Germany.

NOMENCLATURE

$\alpha(t)$	= Coefficient of thermal expansion
α	= Mean coefficient of thermal expansion
τ	= Time
t	= Temperature
$t(x,\tau)$	= Instantaneous temperature
$t(x,\tau_0)$	= Temperature at the moment of restraining
t_A, t_B, t_C, t_0	= Temperatures, explained in Figs. 4 and 5
t_{max}, t_{min}	= Maximum and minimum cycle temperature, respectively
c, c'	= Over-all spring constant of clamping device and specimen train
N	= Cycles-to-failure
n	= Cycle number
$E(t)$	= Modulus of elasticity
ε	= Strain
$\varepsilon_{el}(x,\tau)$	= Elastic strain
$\varepsilon_{pl}(x,\tau)$	= Plastic strain
ε_{pl}	= $\alpha(t_0-t_A)$, plastic strain measured at the first cycle (10^{-3} = 0/00)
ε_l	= $\alpha(t_B-t_C)$, strain equivalent to the width of the loop at the end of the first cycle (10^{-3} = 0/00)
A	= Cross-sectional area of specimen gage length
σ	= Stress = $\frac{LOAD}{A}$
$\sigma(\tau)A$	= Instantaneous load on the specimen
σ_t	= Maximum tensile stress of a cycle
σ_c	= Maximum compressive stress of a cycle
$\sigma_t-\sigma_c$	= Stress range of a cycle

INTRODUCTION

The interest in the thermal fatigue behavior of metals measured by the amount of published papers has taken a sizeable uprise in the past decade. Basically, two distinctly different approaches to the problem can be found.

The first one is more concerned with the qualitative assessment of the thermal fatigue strength and the investigations of metallurgical changes in the specimen during the test. The knowledge of the magnitude of the stresses and strains occurring during these tests is only of secondary importance. Complicated shaped specimens are immersed into a hot and a cold environment, or heated intermittently by high frequency currents while being cooled (1-8). Thermal stresses are created by the temperature gradients and the geometry of the specimen, no external restraint is necessary.

The second approach is used by investigators interested in the magnitude of thermal stresses and strains during thermal fatigue cycling. Coffin (9, 10) was the pioneer of this group. He restrained a cyclically heated and cooled tubular specimen from thermal expansion, and thus generated cyclic thermal stresses. Since the publication of this fundamental contribution, investigators in the U.S.A. (11-14), Japan (15-17) and Russia (18-24) used his method to determine the fatigue strength of heat resistant materials under a variety of conditions. Only recently publications appeared (25-31) showing that the basic Coffin type test could be modified to get more accurate data of the stresses and strains involved in a thermal fatigue test.

It is the purpose of this paper to show one such method of modification, to shed light on the influence of the stiffness of the restraining member and of the moment of restraint on the stresses and strains at the set-up cycle. The influence of these two parameters on the behavior of the specimens during thermal cycling and on the fatigue life will also be discussed.

MATERIAL AND METHOD OF TESTING

Specimens shown in Fig. 1 were subjected to temperature cycles while they were restrained from thermal expansion. Therefore, only thermal stresses are created in the specimen. The chemical composition and the heat treatment of the material Nimonic 80A were:

C	Si	Mn	Cr	Ti	Al	Co	Cu	Fe	Ni
0.07	0.42	0.07	19.4	2.54	1.38	0.71	0.07	0.63	Bal.

Annealed 8 hours at 1080C, air cooled; precipitation hardened 16 hours at 700C, air cooled.

The apparatus for thermal fatigue testing has been described elsewhere in detail (30, 31). It is of the Coffin-Freeman type with some modifications to their original design. It displays the following features:

1. Quick-grip clamping device, so that the thermal expansion of the specimen can be restrained at any point of the temperature cycle. Clamping is achieved by frictional forces between the specimen and the clamping bar, and it is originated by tightening the cross bolts, Figs. 2 and 3.

2. By changing the area of the cross section of the cross bars, the degree of restraint and therefore the severity of stressing can be altered easily, Figs. 2 and 3.

3. Temperature limits are controlled by the thermocouple spot-welded to the center of the gage length.

4. Temperature-reaction force hysteresis loops are read automatically at certain predetermined intervals throughout each test. Thus, accurate thermal stresses and approximate plastic strains in the specimen are known throughout each test.

5. A controller stops the test automatically after the crack has traveled through a major portion of the cross section of the specimen.

All tests were run at a minimum cycle temperature of 200°C. The maximum temperature was varied from test to test in order to get cycles-to-failure in the range 200 to 30,000 cycles. Two types of tests were run. In Series I, tension series, the specimens were clamped at the maximum temperature of the cycle, in Series II, compression series, the specimens were restrained at the minimum cycle temperature. Typical hysteresis loops at the start of a test in Series I and Series II are shown in Fig. 4 and Fig. 5, respectively. It is clear from these figures why the two series have been called tension and compression series. In the first one,

where thermal contraction is constrained, a tensile stress develops first. In the second, thermal expansion is restrained, and a compressive stress builds up in the specimen.

In addition to the moment of clamping, the stiffness of the restraining frame has been varied. Each series was run in two clamping frames. They are characterized by their spring constant which amounts to 13.10^5 kp/cm and $1.67.10^5$ kp/cm, respectively. Tests in the stiff clamping device are designated by an asterisk, I* and II*. Table I shows a survey of the test conditions used.

The test frequency was about 2 cycles/min. Heating was much faster (2.5 sec.) than cooling (25 sec.).

DEFINITIONS

For a temperature cycled restrained specimen, the net elongation has to be zero at every time; this leads to the following expression, see Fig. 6 and Nomenclature.

$$(1)\quad \int_0^{\ell} \left[\varepsilon_{el}(x,\tau) + \varepsilon_{pl}(x,\tau) \right] dx + \int_0^{\ell} \alpha(t) \left[t(x,\tau) - t(x,\tau_0) \right] dx + \frac{\sigma(\tau) A}{C} = 0$$

Due to the uneven temperature distribution along the specimen, the strain varies from section to section. However, the same stress is transmitted through each part. The center of the specimen undergoes the highest temperature, therefore it is the weakest part in the gage length and the plastic deformation concentrates there.

It has been shown in (30, 31) that the plastic strains in the center of the specimen can be determined approximately from the hysteresis loop measurements. The proposed way to calculate the plastic strains is also equal to method I of (25). The specimen design in this study eliminates the correction for the actual gage length.

Any measurement of the plastic strain should show the concentration of the plastic strain in the center of the gage length. Fig. 7 exhibits the condition of maximum plastic strain in the center of the gage length. The results are for a maximum temperature of 600°C and 700°C. This method of determining the plastic strain is only an indirect one. It is not capable of monitoring the changes in the local plastic

strain which may occur under certain conditions due to bulging and necking.

In tests of this type, the temperature is the independent variable. It causes mechanical strains and stresses when the specimen is restrained from thermal expansion. The two series of tests can also be characterized by their integrated mechanical strain which fluctuates in the positive range for Series I, I* and in the compressive range for Series II, II*. Application of Equation (1) to these two cases will prove this statement easily.

In Series I, I* $t_{max}(x) = t(x, \tau_o)$, therefore $t(x,\tau) = t_{min}(x)$ where the maximum integrated mechanical strain occurs

$$(2) \quad \int_0^\ell [\varepsilon_{el}(x) + \varepsilon_{pl}(x)]dx = \int_0^\ell \alpha(t)[t_{max}(x) - t_{min}(x)]dx - \frac{\sigma_t \cdot A}{c}$$

In Series II, II* $t_{min}(x) = t(x, \tau_o)$, therefore $t(x,\tau) = t_{max}(x)$

$$(3) \quad \int_0^\ell [\varepsilon_{el}(x) + \varepsilon_{pl}(x)]dx = -\int_0^\ell \alpha(t)[t_{max}(x) - t_{min}(x)]dx + \frac{|\sigma_c| \cdot A}{c}$$

Based on the initial gage length, the integrated mechanical strain varies between zero and the peak values in Equations (2) and (3). Since the stresses σ_t, σ_c change during cycling, the values of the integrated strains also change. Therefore, a thermal fatigue test of this type does not impose a constant integrated strain limit on a specimen. The independent variable is only the range of the temperature at the center of the specimen gage length.

It is perhaps worthwhile to note that the condition of reversed integrated strain range can also be obtained in a thermal fatigue test by clamping the specimen not at the temperature extremes, but somewhere in between.

THE INFLUENCE OF CLAMPING FRAME STIFFNESS

A. The Stresses and Strains at the Set-Up Cycle

A stiff clamping device imposes more severe duty on the specimen than a weak one. A greater amount of the thermal

strain will be transformed to mechanical strain under these conditions. Equation (1) can be solved for an elastic material easily and we get:

$$(4) \quad \sigma = -\frac{\int_0^\ell \alpha(t)[t(x,\tau) - t(x,\tau_o)]dx}{\int_0^\ell \frac{dx}{E(t)} + \frac{A}{c}}$$

These stresses are due to the restraint only. There is also a self-equilibrating stress system in the test specimen caused by the nonuniform temperature distribution along the specimen gage length shown in Fig. 7. Those stresses, however, are even present in the unrestrained bar and are not affected by the degree of constraint. They will be neglected in the following discussion.

Equation (4) shows that the stress for a given temperature range depends highly on the spring constant c. For $c = \infty$, complete restraint, the highest possible stress develops, for $c = 0$, no restraint, the stress vanishes.

It is also possible to calculate approximately the stresses for the actual material behavior by using plastic strain-stress relationships and temperature dependent material properties, cf. (26). However, no method of calculation is available to account for the shift of the maximum stresses during cycling which will be discussed later.

A good qualitative judgment on the real behavior of the specimen can be obtained from the σ-ε-t plot shown in Fig. 8. In this illustration the stress-strain diagrams at various temperatures are plotted along the t-axis and form a surface. Consider now the ideal case of uniform temperature distribution along the gage length and of two clamping frames C and C' with spring constants c and c'; $c > c'$. If the specimen is restrained from expansion at the minimum temperature of the cycle, the σ-ε-t diagram will be OAB for a test in clamping device C, and O'A'B' for that in C'. On loading, temperature increase, the curve will follow the surface composed of the stress strain diagrams at the various temperatures. The specimen tested in the stiff clamping device will show a greater slope than the specimen tested in the weak one. Points A and A' are somewhere on the stress strain diagram of the maximum temperature of the cycle, σ_A being higher than $\sigma_{A'}$. Unloading, decrease in temperature, takes place along

AB and A'B', respectively. At $\sigma = 0$, points B and B', a certain plastic deformation remains which is, of course, greater for the specimen tested in the stiff clamping frame than for the other specimen. Because of this plastic deformation, a stress of opposite direction, later on called back stress, will develop when the specimen reaches the minimum temperature again. This stress is zero for purely elastic deformation and increases with increasing plastic deformation accumulated during loading. When the elastic limit is exceeded in the opposite direction, a linear relationship between plastic strain and back stress is no longer valid.

In the actual experiment we measure only the projection of the path OAB or OA'B' in the σ,t plane. The hysteresis loops obtained by this method are shown in Figs. 4 and 5 for the conditions of the tension and compression series, respectively. Plastic strains are then calculated from the hysteresis loops via the approximate method given in (30, 31).

The results derived from these measurements show the expected behavior. In Fig. 9 the plastic strain of the first cycle is plotted versus the maximum cycle temperature. Tests in the stiff clamping device show a greater plastic strain at a certain maximum temperature than those in the weak one. The plastic strain at a certain maximum cycle temperature depends also on the moment of restraint. For the compression series, where the stress increases with increasing temperature, the plastic strain is higher than for the tension series, where the stress increases with decreasing temperature. The maximum tensile and compressive stresses at the first cycle are plotted versus ε_{pl} in Fig. 10. The back stresses show the expected linear relationship for small plastic strains, the stress being higher for tests in the stiff clamping device than for those in the weak one. This behavior has to be expected since the same plastic strain is developed at a lower maximum temperature in the stiff frame than in the weak one.

B. The Behavior During Cycling

If cycling is continued, two distinct characteristics can be observed.

Firstly, the maximum stresses generated in the specimen shift and tend to reach an equilibrium position in the σ-ε-t space. Equilibrium condition is reached when completely elastic or equal plastic deformation at the minimum and maximum

cycle temperature occurs. For the stresses, equilibrium is not at equal tensile and compressive stress but rather higher tensile than compressive stress.

Secondly, cyclic straining causes a change in the material properties. This effect is commonly referred to as strain-hardening or strain-softening.

These two mentioned characteristics are affected by the parameters of this investigation. They are also interconnected, since they either depend on the stress-strain diagram (shift of stresses) or influence its shape (change of material property).

The shift of the stresses is primarily caused by the difference in the stress-strain diagram at the minimum and at the maximum cycle temperature. At the same deformation, a higher stress is tolerable at the minimum cycle temperature than at the maximum cycle temperature. The rate of the stress shift (stress change per cycle) is governed by the access plastic deformation at one temperature extreme.

If the boundary conditions are such that the amount of plastic deformation at the temperature extremes is nearly equal, little shift of the stresses is observed. This is demonstrated in Fig. 6 of (29) showing the behavior of specimens of Series I at a maximum temperature of 745°C. If, however, the condition of equal plastic or completely elastic deformation is heavily disturbed at the start of the test, a considerable shift can be observed. It is very pronounced in tests of the compression series. This shift is illustrated in Fig. 11 showing the variation of the stresses during cycling for tests of Series II* at a maximum cycle temperature of 800°C. In Fig. 12 the behavior of specimens of Series I* at the same maximum temperature is illustrated. Note, that despite of differences at the start of the test the values of the stresses toward the end of the test are almost equal for the two series. This is not always true. Sometimes, especially for lower maximum cycle temperatures than 800°C, the beginning fatigue fracture prevents the specimen to reach complete shake-down condition.

The influence of the clamping frame stiffness on the shift of the stresses is illustrated in Fig. 13 for two tests of the compression series at 745°C maximum cycle temperature.

Both tests start out with the same compressive stress, an indication that the stress-strain curve at 745°C is flat, cf. Fig. 8. However, the stiff device introduces initially more plastic deformation than the weak one ($|\varepsilon_B| > |\varepsilon_{B'}|$ in Fig. 8). Therefore, the back stress is higher for Series II* than for Series II. The rate of increase of the tensile stress is about the same for both tests. The access plastic deformation at subsequent cycles for the two tests is about the same, since the maximum temperature and the compressive stresses are equal. The tensile stresses at the minimum cycle temperature are below the yield limit (33) and contribute no plastic deformation. Therefore, the rate of increase of the stresses, governed by the access plastic deformation, should be equal for the two tests.

It is believed that strain-hardening or strain-softening exhibits itself by an increase or a decrease of the stress range during cycling. The increase of the stress amplitude was not very much pronounced and not appreciably affected by the test parameters, cf. Fig. 11, 12, 13. It was only observed up to a maximum cycle temperature of 840°C. Above this temperature, a decrease in the stress amplitude with cycles occurred. At this temperature the fracture mode changed from transcrystalline to intercrystalline (29).

Since the stresses are allowed to change freely during cycling, the magnitude of the tensile stresses shortly before fracture could indicate whether a maximum tensile stress, at which the fatigue fracture would start, does exist. In Fig. 14 the maximum stresses shortly before fracture are plotted versus the maximum cycle temperature. It is evident that no maximum tensile stress exists under these conditions. Orowan's theory (32) seems, therefore, not applicable for these thermal fatigue tests.

C. The Fatigue Life

Before comparing the fatigue life of the specimens in the two clamping devices, a short description of how these tests differ from conventional fatigue tests is necessary.

In a standard fatigue test, the maximum and the minimum stress of a cycle are kept constant throughout each test and the number of cycles-to-failure is noted. In the final representation the maximum stress (or stress amplitude) is

plotted versus cycles-to-failure and we get the well known S-N curve. Under these conditions usually the high-cycle end of the S-N curve is of interest. Stresses are within the technical elastic limit.

In this type of thermal fatigue test, the maximum temperature at the center is the independent variable. Also, the conditions are such that plastic deformation will occur at each cycle. The material properties and the conditions at the specimen-clamping device boundary, together with this maximum temperature, determine the temperature distribution along the gage length and hence the distribution of the strain and the resulting thermal stresses. Strains and stresses are therefore dependent values. If the material properties change, these values change accordingly. This has been shown in the previous section.

In order to compare dependent variables in a S-N type diagram, each point should be taken at the same degree of damage of the individual specimen. Since the rate of damage increase during cycling is not known, it is difficult to find such a common point. At the first cycle, however, the damage is at the very start, and all specimens are in the same condition. Since cyclic plastic strain changes the stress-strain diagram of the material, exhibited by strain-hardening or strain-softening, values taken at the start of the test are much more related to the monotonic stress-strain curve on which all the engineering data are based. It is possible that during thermal cycling the stress range increases about 20%, (10). Associated with this phenomenon, is a corresponding increase in the yield strength. The material is, therefore, no longer in its initial condition and it is not feasible to treat it as if it was still the same. To avoid this difficulty it is tentatively proposed to compare dependent values at the first cycle or at least very early in the specimen life.

In Fig. 15 the independent variable of the four series, the maximum temperature is plotted versus the number of cycles-to-failure. It is evident from this illustration that the specimens in the stiff device exhibit a shorter fatigue life than those in the weak one. The specimens in the weak clamping frame also show the influence of the moment of clamping, specimens of the tension series showing a shorter life than those of the compression series. This effect is wiped out in the stiff device where all the data can be

represented by one line. It is possible that the scatter covers an existing small effect. The curves show the same character as those shown in (19), the effect of the clamping frame stiffness on cycles-to-failure seems to be somewhat smaller for Nimonic 80A than for the materials tested in (19), (EI437B is the Russian equivalent to Nimonic 80A). At a stiffness ratio (c'/c) of 0.27 the fatigue life differs almost by a factor of 10 in (19). In this case the stiffness ratio is 0.12, and the fatigue life is different by a factor of approximately 5.

The slope of the lines is about the same in both cases, about 120°C per order of magnitude. It is also evident from Fig. 3 in (19) and from Fig. 15 of this investigation, that the slope becomes somewhat steeper with increasing clamping frame stiffness.

Figs. 16, 17, 18 and 19 show the dependent variables plotted versus number of cycles-to-failure. As mentioned before these dependent values are determined at the first cycle, they are defined in the Nomenclature and in Figs. 4 and 5. With the exception of the stresses (Figs. 17, 18), the usual linear relationship between ordinate and cycles-to-failure, both on logarithmic coordinates, is shown. The relationship for the stresses is due to the characteristic variation of the stress-strain curves with temperature, Fig. 8. Since the strength properties decrease with increasing temperature for almost every material, this type of curve should be expected every time. It is interesting to note that all the points for the width of hysteresis loop versus cycles fall on one curve which is straight initially, Fig. 19. Similar observations have been made by other investigators (26, 34, 35) for thermal and isothermal low cycle fatigue conditions leading to the suggestion that this quantity is very important in low cycle fatigue.

To assess the resistance of materials against thermal-stress fatigue under varying boundary conditions, dependent variables have to be clearly separated from independent ones. Only the independent variable will indicate the influence of the parameter under investigation on the fatigue life. At present this is the only safe way to assess the performance of materials under various conditions of thermal fatigue cycling. This can only be done on a relative basis, no absolute method is available.

When dependent variables are used to determine the fatigue life an erroneous conclusion is very likely. For example, if Fig. 18 would be used as it is common for a S-N diagram one would arrive at the statement that tests in the stiff clamping device would lead to longer life than those in the weak one. This statement is obviously incorrect

A comparison of the fatigue life on the basis of the plastic strain, Fig. 16, would show that, depending on the magnitude of $\varepsilon_{p\ell}$ involved, tests in the weak device would last longer than those in the stiff one and vice versa, results which contradict the conclusions from Fig. 18. Both predictions, however, do give an erroneous picture of the actual behavior.

The value of a unique fatigue curve of the type shown in Fig. 19, if such a thing exists at all, would be in the fact that a measure for the basic fatigue phenomenon under conditions of cyclic plastic deformation would have been found. An analysis which is still to be developed could then calculate all the different conditions of stress, strain and temperature leading to the same cyclic plastic strain and hence to the same fatigue life. Both the unique fatigue curve and the corresponding analysis will be hopefully developed in the future.

CONCLUSIONS

1) The thermal fatigue apparatus was very well suited for studying the influence of different degrees of constraint on the behavior of the specimens during cycling and on their thermal fatigue life. Reaction force-temperature hysteresis loop measurements at adjustable preset cycle intervals recorded the behavior of each specimen accurately.

2) Two distinct characteristics can be observed during thermal cycling of Nimonic 80A. Both are dependent on or affect the stress-strain diagram of the material.

The maximum stresses shift and tend to reach a shake-down condition. This condition is completely elastic or equal plastic deformation at the temperature extremes. It is not equal maximum compressive and tensile stress but rather greater tensile than compressive stress.

The stress range increases or decreases which is believed to be an indication of the strain-hardening or strain-softening of the material. At 840°C maximum cycle temperature a transition from strain-hardening to strain-softening and from transcrystalline to intercrystalline fracture takes place.

3) The rate of change of the maximum tensile and compressive stress to reach shake-down depends on the minimum and maximum cycle temperature, the moment of clamping, the degree of constraint and, of course, on the material. The changes mostly take place early in the life of a specimen. In some cases the beginning fatigue fracture prevents the specimen from reaching the final equilibrium position.

4) There is no maximum tensile stress which depends on the temperature only and after which the fatigue fracture starts (strain-hardening theory). At a certain maximum cycle temperature the specimens fracture at different maximum tensile stresses under the conditions tested.

5) It is necessary to discern between independent and dependent quantities when cycles-to-failure curves are established. Independent quantities are externally prescribed, in our case the temperature. Dependent quantities, in this case, stresses and strains change during the test according to the conditions imposed by the independent quantities, the material properties and the boundary conditions. When cycles-to-failure curves are established with dependent quantities all specimens have to be compared at the same conditions. It is tentatively recommended to use the first cycle as a reference point for dependent quantities.

6) The influence of a changed parameter of testing, e.g. the spring constant of the clamping device, can only be assessed on the basis of the independent quantity. An increase of the spring constant by a factor 8 reduces the fatigue life to about 0.2 of its initial value. The use of cycles-to-failure curves based on dependent variables would lead to erroneous conclusions.

7) The width of the hysteresis loop at the end of the first cycle is the only quantity which yields one cycles-to-failure curve. It seems to be a prospective candidate for a thermal fatigue criterion.

ACKNOWLEDGEMENT

The work reported in this paper was sponsored by the United States Air Force, Air Force Materials Laboratory, Research and Technology Division, Wright Patterson Air Force Base, Ohio, through its European Office at the Mechanisch-Technisches Laboratorium, Technische Hochschule Muenchen, Germany, Director, Prof. Dr. Dr. H. Neuber. The continuing interest and support of Mr. W. J. Trapp, Air Force Materials Laboratory, is gratefully acknowledged.

BIBLIOGRAPHY

(1) Glenny, E., J. E. Northwood, S. W. K. Shaw, T. A. Taylor, J. Inst. Metals 87 (1959), p. 294/302.

(2) Glenny, E., T. A. Taylor, J. Inst. Metals 88 (1960), p. 449/461.

(3) Northcott, L., H. G. Baron, J. Iron Steel Inst. 184 (1956), p. 385.

(4) Franklin, A. W., J. Heslop, R. A. Smith, J. Inst. Metals 92 (1963), p. 313/322.

(5) Tidball, R. A., M. M. Shrut, Trans. ASME 76 (1954), p. 639/643.

(6) Raedeker, W., Stahl und Eisen 74 (1954), p. 929/943.

(7) Raedeker, W., Stahl und Eisen 75 (1955), p. 1252/1263.

(8) Eichhorn, F., Stahl und Eisen 80 (1960), p. 1275/1283.

(9) Coffin, L. F., R. P. Wesley, Trans. ASME 76 (1954), p. 923/930.

(10) Coffin, L. F., Trans. ASME 76 (1954), p. 931/950.

(11) Clauss, F. J., J. W. Freeman, NACA TN 4160 and 4165, 1958.

(12) Clauss, F. J., NACA TN D69, 1959.

(13) Mehringer, F. J., R. P. Felgar, Trans. ASME, Series D, 82 (1960), p. 661/670.

(14) Majors, H., Jr., Bureau of Eng. Research, Univ. of Alabama, Final Report 1957.

(15) Taira, S., M. Ohnami, T. Kyogoku, Bull. JSME, 6 (1963), p. 178/185.

(16) Taira, S., M. Ohnami, Proc. Fourth Jap. Congress Test. Materials, 1961, p. 45/49.

(17) Miki, H., M. Sugimori, Proc. Sixth Jap. Congress Test. Materials, 1963, p. 47/50.

(18) Serensen, S. V., P. I. Kotov, Industrial Lab., 25 (1959), p. 1272/1279.

(19) Serensen, S. V., P. I. Kotov, Industrial Lab., 28 (1962), p. 1312/1316.

(20) Sobolev, N. D., V. I. Egorov, Industrial Lab., 28 (1962), p. 1317/1321.

(21) Egorov, V. I., N. D. Sobolev, Industrial Lab., 29 (1963), p. 790/793.

(22) Mozharovskii, N. S., Industrial Lab., 29 (1963), p. 794/797.

(23) Balandin, T. F., Industrial Lab., 29 (1963), p. 797/799.

(24) Sklyarov, N. M., Editor, Thermal Fatigue of Heat Resistant Alloys, Moskow 1962. Translated in Foreign Technology Division, WP-AFB, Ohio, Report FTD-TT-63-147/1/2, Sept. 1963.

(25) Carden, A. E., Proc. ASTM, 63 (1963), p. 735/758.

(26) Carden, A. E., ASME Paper 64-MET-2.

(27) Carden, A. E., ASME Paper 65-GTP-5.

(28) Horton, K. E., J. M. Hallander, D. D. Foley, ASME Paper 65-GTP-13.

(29) Krempl, E., Materialpruefung 5 (1963), p. 274/283.

(30) Krempl, E., Materialpruefung 5 (1963), p. 144/153.

(31) Neuber, H., E. Krempl, Air Force ML-TR-65-25, 1965.

(32) Orowan, E., Proc. Roy. Soc., London, A171 (1939), Nr. 944, p. 79/106.

(33) Betteridge, W., The Nimonic Alloys, London, Edward Arnold 1959.

(34) Taira, S. in "High Temperature Structures and Materials", Proc. of the Third Symposium on Naval Structural Mechanics, p. 187/213, Pergamon Press 1964.

(35) Coffin, L. F., Jr. in "Internal Stresses and Fatigue in Metals", p. 365/381, Amsterdam, London, New York, Princeton, 1959.

TABLE I

TEST CONDITIONS

Designation	t_{min} °C	t_{max} varied between °C	Thermal expansion restrained at	Spring constant of clamping frame used kp/cm
Series I	200	715-900	t_{max}	$1.67.10^5$
Series I*	200	720-880	t_{max}	13.10^5
Series II	200	720-925	t_{min}	$1.67.10^5$
Series II*	200	680-890	t_{min}	13.10^5

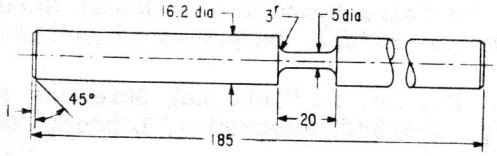

Fig. 1 Test specimen.

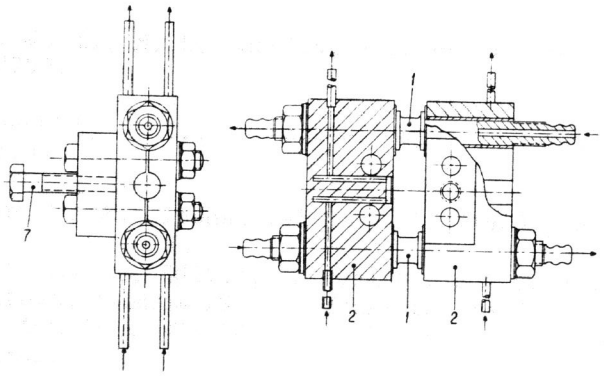

Fig.2 Stiff clamping device, half actual size. Arrows indicate direction of flow of cooling water. c = 13.10^5 kp/cm.
1 = weighbars, shielded in Fig. 3
2 = cross bars
3 = thermocouple
4 = specimen
5 = power terminals
6 = controller leads
7 = quick gripping bolt

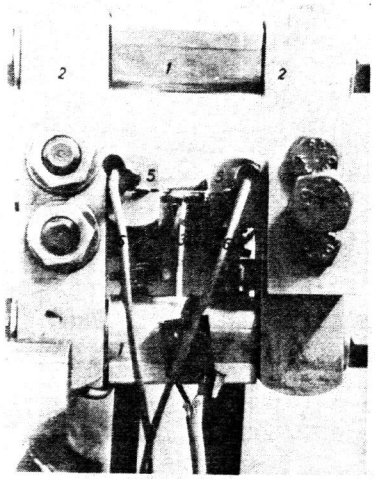

Fig. 3 Weak clamping device in operation, actual size.c' = $1.67.10^5$ kp/cm. Legend, see Fig. 2.

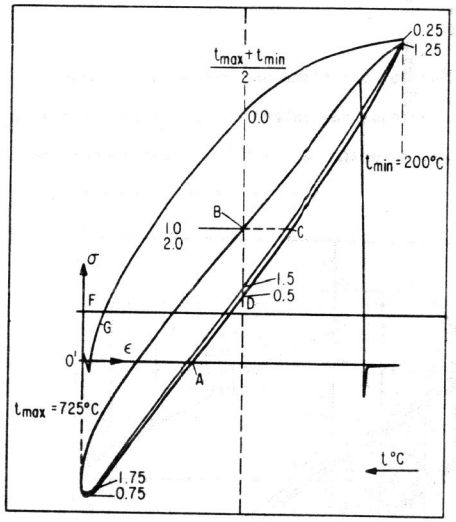

Fig. 4 First hysteresis loop of a Nimonic 80A specimen of Series I*. Maximum temperature 725°C. Original record.

O'A = distance proportional to the strain $\varepsilon_{p\ell}$ of the first cycle

BC = distance proportional to the strain ε_{ℓ} of the first cycle

G = clamping finished

O'F = clamping effect compensation

E = control line (shown only in Fig. 5)

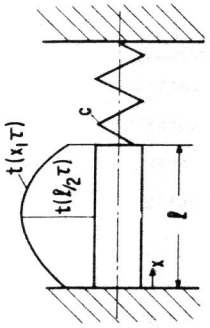

Fig. 6 Schematic representation of the conditions of a thermal fatigue test. Spring (spring constant c) represents elasticity of clamping frame and specimen train.

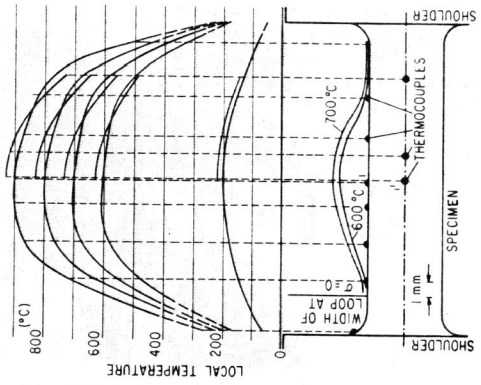

Fig. 7 The variation of the maximum and minimum temperature and of the width of the loop at $\sigma = 0$ along the specimen gage length for various maximum temperatures.

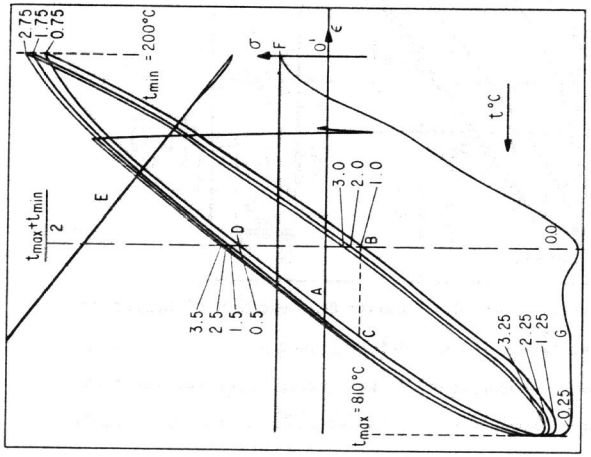

Fig. 5 First hysteresis loop of a Nimonic 80A specimen of Series II*. Maximum temperature 810°C. Legend, see Fig. 4.

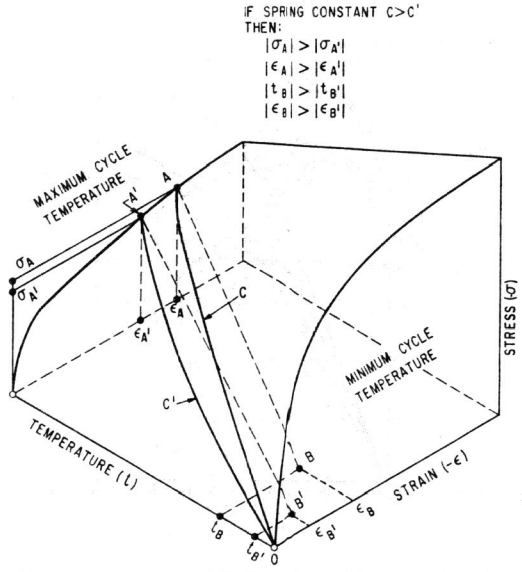

Fig. 8 σ-ε-t space. OAB shows schematic path of temperature, stress and strain under high restraint for loading and unloading. Primed quantities are for a low degree of restraint.
ε_B, $\varepsilon_{B'}$ plastic strain for $\sigma = 0$.
t_B, $t_{B'}$ temperature at $\sigma = 0$.

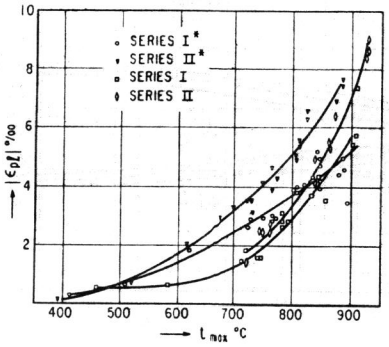

Fig. 9 Plastic strain ($\varepsilon_{p\ell}$) at the first cycle versus maximum cycle temperature (t_{max}).

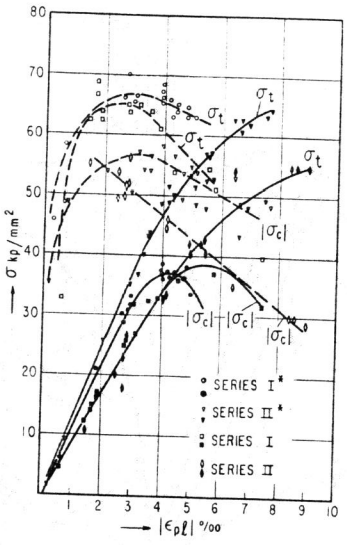

Fig.10 Maximum tensile (σ_t) and maximum compressive stress (σ_c) at the first cycle versus plastic strain ($\varepsilon_{p\ell}$) at the first cycle.

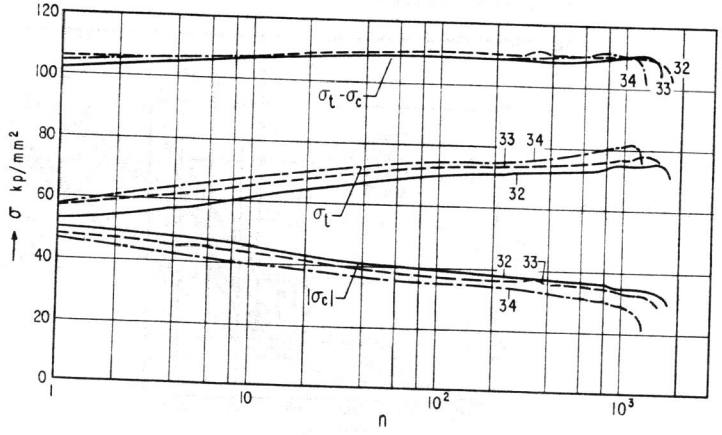

Fig.11 Variation of the stresses during thermal cycling. Maximum temperature 800°C. Series II*.

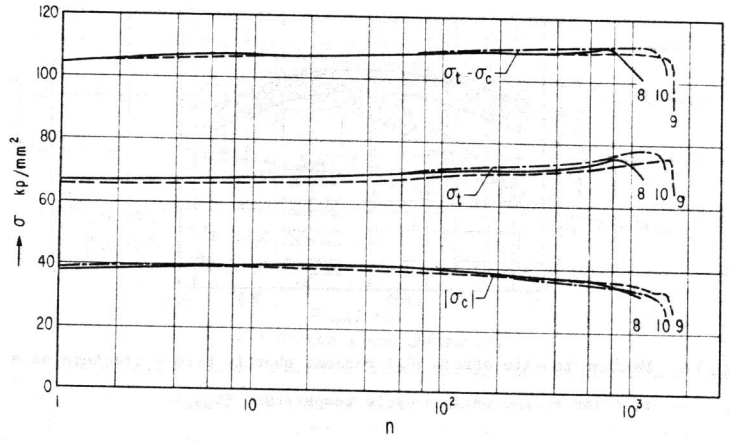

Fig.12 Variation of the stresses during thermal cycling. Maximum temperature 800°C. Series I*.

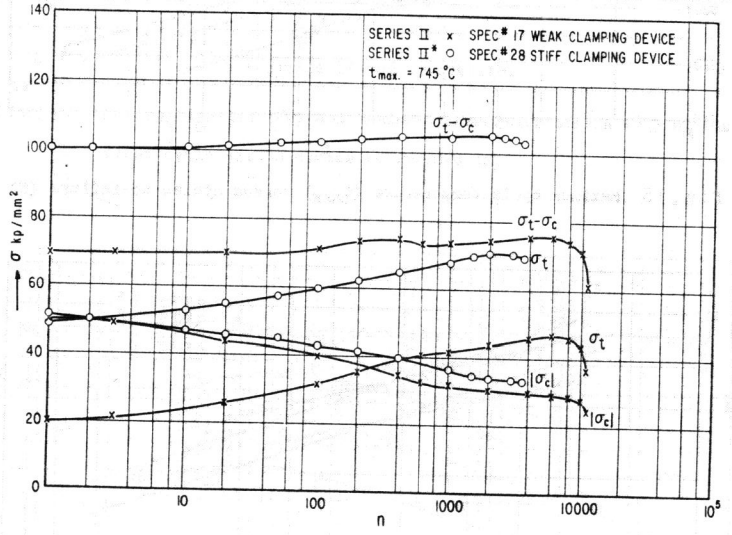

Fig.13 Comparison of the variation of the stresses during thermal cycling for the weak and the stiff clamping device. Series II & II*. Maximum temperature 745°C.

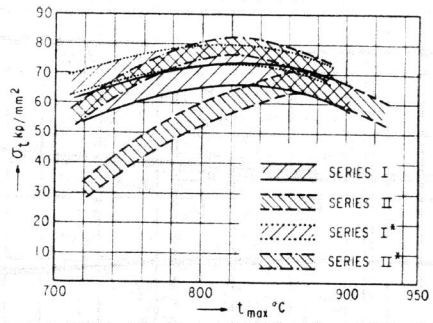

Fig.14 Maximum tensile stress (σ_t) reached shortly before fracture as a function of the maximum cycle temperature (t_{max}).

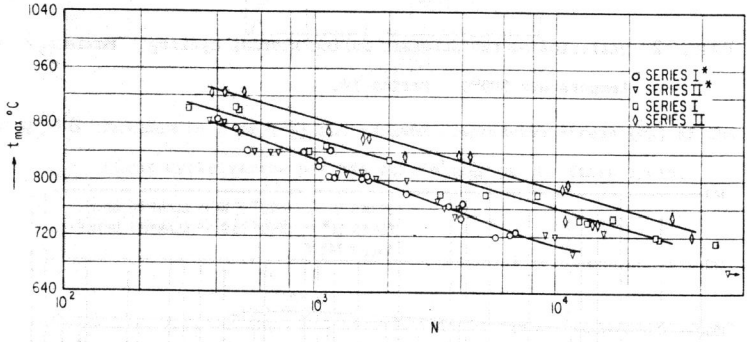

Fig.15 Maximum cycle temperature (t_{max}) versus cycles-to-failure (N).

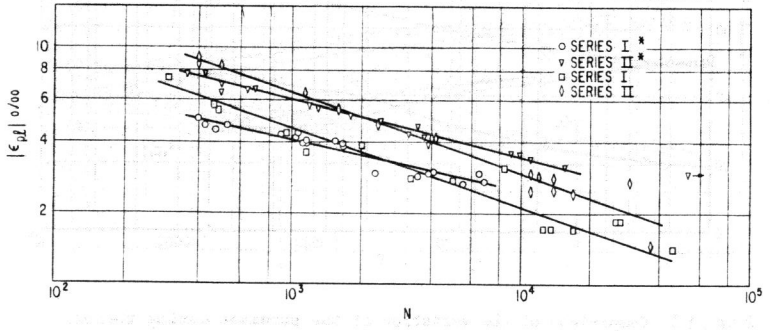

Fig.16 Plastic strain (ϵ_{pl}) at the first cycle versus cycles-to-failure (N).

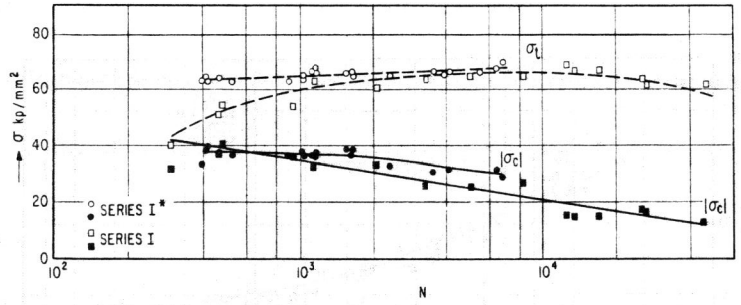

a = Series I and Series I*.

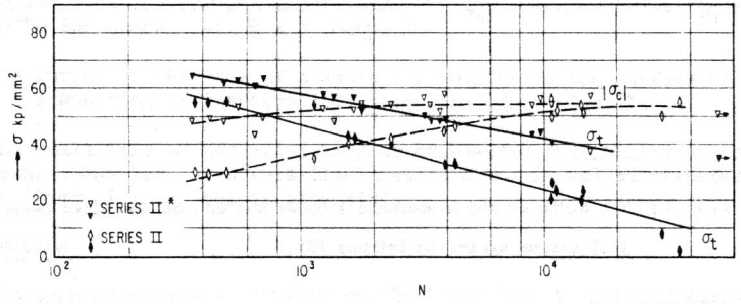

b = Series II and Series II*.

Fig.17 Maximum tensile (σ_t) and maximum compressive stress (σ_c) at the first cycle versus cycles-to-failure (N).

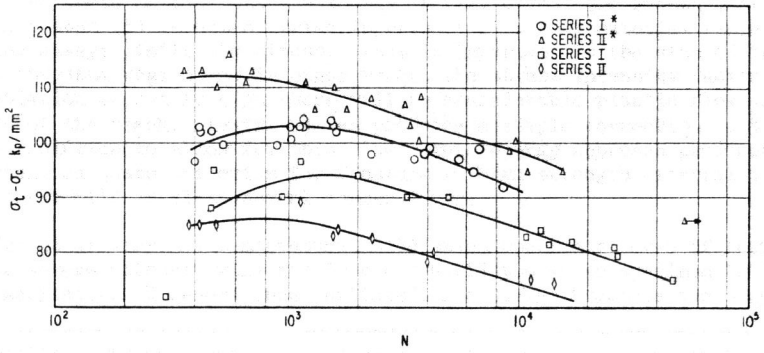

Fig.18 Stress range ($\sigma_t - \sigma_c$) at the first cycle versus cycles-to-failure (N).

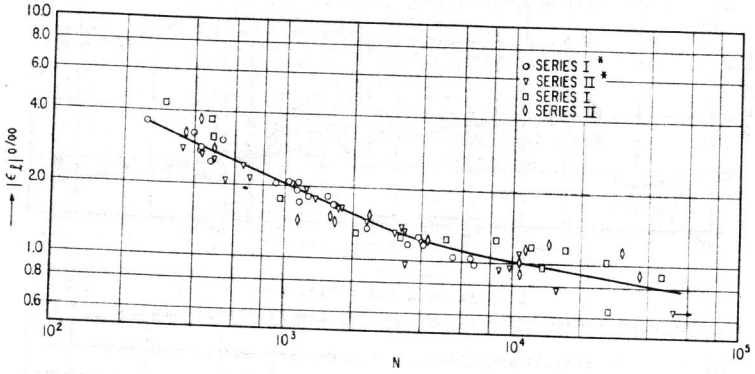

Fig.19 The width of the hysteresis loop at the end of the first cycle (ε_ℓ) versus cycles-to-failure (N).